ISSN 1066-3622, Radiochemistry, 2008, Vol. 50, No. 5, pp. 523–529. © Pleiades Publishing, Inc., 2008.
Original Russian Text © A.N. Veleshko, E.V. Rumyantseva, I.E. Veleshko, A.Yu. Teterin, K.I. Maslakov, Yu.A. Teterin, S.A. Kulyukhin, G.A. Vikhoreva, 2008, published in Radiokhimiya, 2008, Vol. 50, No. 5, pp. 454–459.

X-ray Photoelectron Study of Complexation between Uranyl Group and Chitosan

A. N. Veleshko[a], E. V. Rumyantseva[b], I. E. Veleshko[a], A. Yu. Teterin[a], K. I. Maslakov[a], Yu. A. Teterin[a], S. A. Kulyukhin[c], and G. A. Vikhoreva[b]

[a] *Russian Research Centre Kurchatov Institute, Moscow, Russia*
[b] *Kosygin Moscow State Textile University, Moscow, Russia*
[c] *Frumkin Institute of Physical Chemistry and Electrochemistry, Russian Academy of Sciences, Moscow, Russia*

Received April 4, 2008

Abstract—The interaction of U with chitosan in sorption of U(VI) from sulfate solutions was examined by X-ray photoelectron spectroscopy. It was found that uranyl complexes are formed on the chitosan surface. They contain in the equatorial plane the nitrogen atom of the amino group, as well as, probably, oxygen atoms from the chitosan ring and free hydroxy groups. Prolonged exposure of the chitosan–U(VI) complex in a vacuum chamber of the spectrometer results in cleavage of the bonds linking the uranyl groups with amino and hydroxy groups, which is responsible for formation of U(IV) compounds on the surface with surface depletion in OH groups.

PACS numbers: 82.80.Pv
DOI: 10.1134/S106636220805015 9

Uranium is typically recovered from natural and mine waters by sorption with various sorbents [1–5]. In most cases the examined uranium solutions contained SO_4^{2-} ions [6]. Since recently, special attention has been given to preparation and study of the physicochemical properties of new sorbents based on natural biopolymers chitin and chitosan. These materials exhibit high sorption power with respect to various metals and radionuclides [3–5, 7]. They are suitable for preparation of sorbents in the form of gels, sponges, films, and granules. Low ash content and good biodegradability enable waste compaction.

Our previous study [8] was focused on U(VI) sorption from aqueous solutions of UO_2SO_4 on spherically granulated chitosan. We found that the best sorption and kinetic characteristics were exhibited by freshly formed and cross-linked chitosan granules. The total static exchange capacity of the freshly formed granules was 0.7 mmol of U(VI) per gram of dry sorbent. Based on the calculated diffusion coefficients and the similarity criteria describing the diffusion process parameters, we presumed that, irrespective of the method by which the granules were prepared (freshly formed, cross-linked, air-dry), the dominating process is U(VI) sorption on the surface, mainly controlled by external diffusion. In the presence of SO_4^{2-}, interaction of U(VI) with amino groups of chitosan can occur simultaneously with the complexation between UO_2^{2+} and SO_4^{2-}, with the resulting complexes participating in cross-linking of the amino groups of chitosan.

We examined here the complexation between U(VI) and chitosan by X-ray photoelectron spectroscopy in order to elucidate the U(VI) sorption mechanism.

EXPERIMENTAL

We used freshly formed chitosan granules (FSCG), 3 mm in diameter, prepared by the technique described in [9]. For electron microscopic image of the granules, see [8].

The samples for X-ray photoelectron spectroscopic (XPS) examinations were obtained by the following procedure.

Sample no. 1 (film) was prepared by U(VI) sorption from 1.55 mM UO_2SO_4 solution on the freshly formed granulated chitosan (molecular weight MW = 170 kDa) for 1 h at the solid to liquid phase ratio V/m of 125 and pH 5. Then the granules were separated from the solution, washed with a dilute

(~0.001 M) HNO_3 solution, and air-dried. The moisture content of air-dry granules was 6–8%. To prepare a film, the granules were dissolved in acetic acid (~0.2 ml of 3–6% CH_3COOH), and the resulting solution was applied to an aluminum substrate and air-dried. This yielded a ~5-μm thick film containing ~5–8 mg of U(VI).

The film preparation was accompanied by the following reaction:

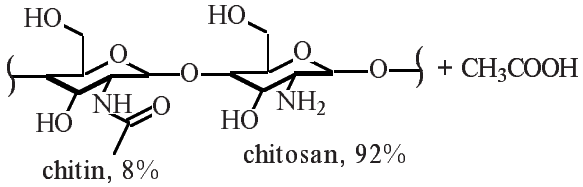

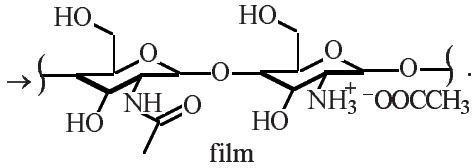

Sample no. 2 (powder). Sorption of U(VI) on a freshly formed granulated chitosan (MW = 170 kDa) followed the procedure described above for sample no. 1. Then the granules were separated from the solution, washed with a dilute (~0.001 M) HNO_3 solution, and air-dried. The moisture content of the air-dry granules was 6–8%. To prepare a powder, the granules were milled in a ball mill into particles ~20 μm in diameter. The U content of the powder was 46 mg of U(VI) per gram of the material.

Preparation of granules for uranium sorption was accompanied by the following reaction:

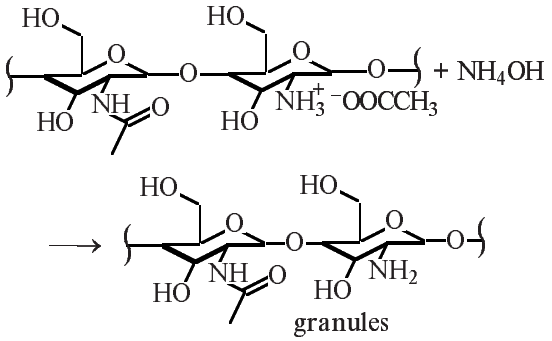

$+ CH_3COONH_4 + H_2O.$

Sample no. 3 (powder) was a chitosan powder prepared by milling of air-dry granules in a ball mill to particles ~20 μm in diameter.

Sample no. 4 (powder) was a powdered chitosan–U(VI) complex. Sorption of U(VI) on the powdered chitosan (MW = 170 kDa) followed the procedure described above for sample nos. 1 and 2. The powder was prepared from air-dry granules by milling in a ball mill into particles ~20 μm in diameter. After the sorption, powdered chitosan was separated from the solution by centrifugation, washed with ~0.001 M HNO_3 solution, and air-dried.

Sample no. 5 (powder) was 0.5 g of powdered $UO_2SO_4 \cdot nH_2O$, prepared by $UO_2(OH)_2$ precipitation with NH_4OH from a $UO_2SO_4 \cdot 3H_2O$ solution, which was followed by dissolution of $UO_2(OH)_2$ in 1–3 M H_2SO_4. The solution was evaporated to wet salts and then exhaustively dried in air at 30°C. The dry residue wax thrice washed with C_2H_5OH and air-dried. The salt of the composition $UO_2SO_4 \cdot nH_2O$ was ground in a porcelain mortar.

The X-ray photoelectron spectra were measured on an MK II VG Scientific electrostatic spectrometer with $AlK_{\alpha_{1,2}}$ (1486.6 eV) nonmonochromated X-ray excitation radiation in a 1.3×10^{-7} Pa vacuum at room temperature. The resolution of the spectrometers, measured as the half-width of the line of Au $4f_{7/2}$ electrons, was 1.2 eV. The binding energies of the electrons E_b, eV, are referenced to that of C 1*s* electrons of hydrocarbons on the surface of the samples (saturated hydrocarbons), taken as 285.0 eV. The binding energies E_b, eV, and line widths Γ, eV, of the electrons were measured accurately to within 0.1 eV, and relative intensities, accurately to within 10%. The line halfwidths are calibrated relative to the corresponding parameter of the line of C 1*s* electrons, Γ(C 1*s*) = 1.3 eV.

For measuring the X-ray photoelectron spectra, samples in the form of finely ground powders were pressed into a two-sided conducting adhesive tape. In all cases, we recorded the spectra of the valence band electrons within 0–50 eV; U 4*f* electrons; N 1*s* electrons; and O 1*s* and C 1*s* electrons of oxygen and carbon. The spectra of the U 4*f* electrons allow determination of the valence of the uranium ions. The samples get strongly charged (to 5 eV in the binding energy of the electrons), and such charging is unstable in time. For this reason, the spectra were calibrated relative to the line of carbon for each separate line, rather than for the entire spectrum within the 0–1000 eV energy range. In other words, the line of the spectrum of the C 1*s* electrons was measured before and after recording the target line of the element. This allowed the error in determining the binding energy of the electrons of the elements in the samples examined to be decreased to 0.1 eV. Sample nos. 1–3 after the initial examination were

Electron binding energies E_b, eV, of the compounds and complexes (figures in parentheses are the binding energies for electrons and shake-up satellites)

Material	$U^{4+}4f_{7/2}$	$U^{6+}4f_{7/2}$	N 1*s*	S 2*p*	O 1*s*	C 1*s*
Sample no. 1a	380.3 (1.5)	382.3 (1.5)	399.4 (1.5), 401.6	–	532.7 (2.4)	285.0 (1.3), 286.7, 288.4
Sample no. 1b	380.7 (1.5)	382.5 (1.5)	399.9 (1.7), 401.6	–	532.4 (2.4)	285.0 (1.3), 286.7, 288.3
Sample no. 2a	380.7 (1.5)	382.4 (1.5)	400.1 (1.5), 401.5	–	531.3 (1.5), 533.1	285.0 (1.3), 286.5, 288.2
Sample no. 2b	380.8 (1.5)	382.5 (1.5)	399.7 (1.5), 401.9	–	531.4 (1.5), 533.1	285.0 (1.3), 286.6, 288.2
Sample no. 3a	–	–	399.6 (1.3)	–	533.2 (1.5)	285.0 (1.3), 286.5, 288.2
Sample no. 3b	–	–	399.7 (1.2)	–	533.2 (1.3)	285.0 (1.3), 286.5, 288.2
Sample no. 4	380.7 (1.4)	382.3 (1.4)	399.7 (1.2), 401.9	160.5 (1.3), 165.8	531.3 (1.4), 533.0	285.0 (1.3), 286.6, 288.4
Sample no. 5	–	383.1 (1.8), 385.9 sat	–	169.6 (1.9)	532.4 (1.5)	285.0 (1.3)
Chitosan [16]			399.9			
Chitin [16]			401.6			
UO_2 [12]	380.9				530.5	285.0
γ-UO_3 [12]		382.4			531.4	285.0
Cellulose [13]					532.5	

left in the spectrometer for 1 day, after which they were examined once again to elucidate how their stability is affected by a high vacuum in the spectrometer. For this reason, we introduced the following designations: nos. 1a–3a and 1b–3b for the samples examined on the first and second day, respectively (see table).

All the samples were subjected to quantitative elemental and ionic analyses underlain by the proportionality between the spectral line intensity and the concentration of the atoms in the sample analyzed. Such analysis was based on the following relationship:

$$n_i/n_j = (S_i/S_j)(k_j/k_i), \quad (1)$$

where n_i/n_j is the relative concentration of the target atoms; S_i/S_j, relative intensity of the lines of the inner-shell electrons of these atoms; and k_j/k_i, experimental relative sensitivity coefficient. We used here the following values of these coefficients relative to carbon: 1.00 (C 1*s*), 2.64 (O 1*s*), 1.68 (N 1*s*), 36.0 (U $4f_{7/2}$), 2.16 (S 2*p*) [10].

RESULTS AND DISCUSSION

The configuration of the valence electrons and the ground spectroscopic state of the U atom can be represented as $_{92}U6s^26p^65f^36d7s^2$ and $^5L_6^0$, respectively. Hence, U can exist in several oxidation states; UO_2 and UO_3 belong to the most stable oxides. For these oxides, the electron binding energies E_b, eV, of different shells are known, like in the case of metal. For example, the U 4*f* electrons in the X-ray photoelectron spectra exhibit a doublet due to spin–orbit interaction with the splitting ΔE_{sl} = 10.8 eV [11]. The spectrum of these electrons contains satellites characteristic for different oxidations states of U on the higher-energy side of the main lines at ΔE_s. For example, the U $4f_{7/2}$ electrons are characterized by E_b for U (metal), UO_2, and γ-UO_3 of 377.4 (ΔE_{sl} = 10.8 eV [11]), 380.9 (ΔE_s = 6.9 eV [12]), and 382.4 eV (ΔE_s = 3.7 eV [12]), respectively. For U, the binding energies of electrons of other levels in various compounds are known [12].

The X-ray photoelectron spectra of the examined samples of chitosan and its complexes with U(VI) at electron binding energies within 0–1200 eV contain lines associated with their constituting elements, as well as Auger spectral lines of carbon (C *KVV*) and oxygen (O *KVV*) (Fig. 1a). This energy range can be conventionally divided into three regions [12]. The first region corresponding to electron binding energies within 0–15 eV exhibits a structure associated mainly with electrons from outer valence molecular orbitals (OVMOs), to which U 5*f*, U 6*d*, U 7*s*, C 2*p*, O 2*p*, and N 2*p* electrons of the outer valence atomic shells strongly contribute (Fig. 1b). In this spectral region, the intensity of the line at E_b = 1.9 eV, associated with U 5*f* electrons not involved in chemical bonding, serves as a quantitative characteristic of the ionic composition of uranium in a substance [12]. The second energy region, 15–

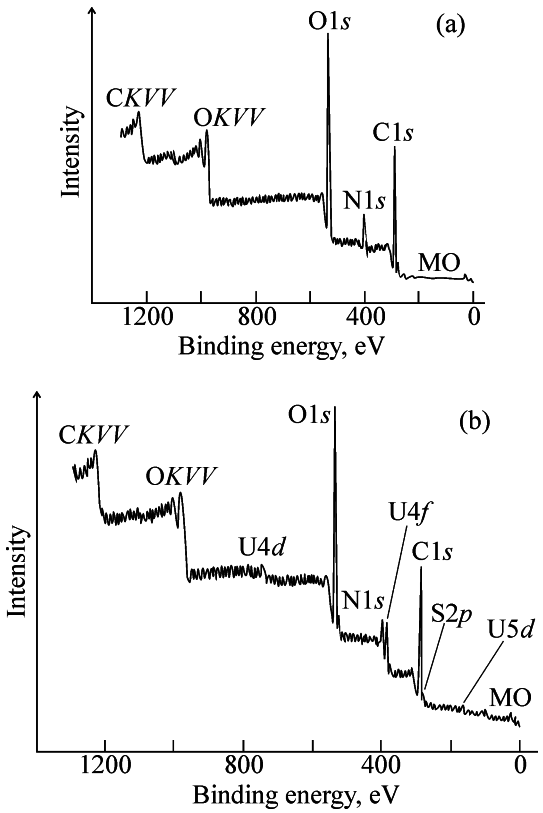

Fig. 1. Survey X-ray photoelectron spectra of sample no. (a) 3a and (b) 4.

50 eV, exhibits a structure associated mostly with electrons from inner valence molecular orbitals (IVMOs), mainly with electrons from low-energy completely filled U 6*p*, C 2*s*, O 2*s*, and N 2*s* inner valence shells of the neighboring atoms. The characteristics of this structure correlate with the parameters of the structure of the nearest surrounding of the U(VI) ions in complexes and compounds [13]. The third energy region, ≥50 eV, exhibits a structure of the spectra of the inner (core) electrons weakly involved in formation of inner molecular orbitals (CMOs), which are virtually completely neglected in discussion of the X-ray photoelectron spectra. However, the spectrum in this region can exhibit a structure due to spin–orbit interaction with the splitting ΔE_{sl}, eV, as well as to multiplet splitting ΔE_{ms}, eV, multielectron excitation, dynamic effect, etc. [12]. The parameters of this structure characterize different properties of compounds and hence are used in combination with such conventional characteristics as electron binding energy and chemical shifts of levels and their separations, as well as the spectral line intensity. For simplicity, in further discussion we will utilize both the molecular and atomic terms and designations.

Spectra of low-energy electrons (0–50 eV). The low-energy region in the spectra of the surface of the examined complexes contains lines of U 5*f* electrons and electrons from OVMOs, associated with outer valence U 5*f*, U 6*d*, U 7*s*, C 2*p*, O 2*p*, and N 2*p* electrons, as well as a structure associated with electrons from IVMOs, associated with U 6*p*, C 2*s*, O 2*s*, and N 2*s* electrons. The energy region corresponding to O 2*s* electrons of the examined samples exhibits a broad structured line. For chitosan (sample no. 3), this line has a width Γ of 4 eV, while the line of the O 1*s* electrons is much narrower (Γ ≈ 1.5 eV). The structure in the region of the binding energies of O2*s* electrons is associated with formation of IVMOs. The spectral lines of the U 5*f* and U 6*p* electrons are fairly weak, which complicates correct elemental and structural analyses on the basis of their intensities and splittings. However, the structure of the spectra of low-energy electrons allows some qualitative conclusions which, as we will demonstrate below, agree with the data derived from the spectra of inner electrons. Indeed, the spectrum of low-energy electrons of chitosan (sample no. 3) upon 1-day exposure to a high vacuum in the measuring chamber of the spectrometer did not change appreciably. At the same time, in the spectra of these electrons in the chitosan–U(VI) complexes (sample nos. 1 and 2), the line of U 5*f* electrons substantially increased in intensity. This suggests a decrease in the number of the U^{6+} ions on the surface of the samples and an increase in that of the U^{4+} ions. The spectrum of the chitosan–U(VI) complex (sample no. 4) also contains the line of the U 5*f* electrons. Such analysis is possible, since only the line of U 5*f* electrons is observed in the spectra of the examined substances (dielectrics) at the electron binding energy of 1.9 eV, and any other lines are absent.

Spectra of inner electrons (E_b ≥ 50 eV). Elemental and ionic quantitative analyses of the samples by XPS typically utilize the most intense lines of their constituting elements [13]. For the compounds of interest we chose the lines of C 1*s*, O 1*s*, N 1*s*, S 2*p*, and U 4*f* electrons (see table). The spectra of S 2*p* and U 4*f* electrons are represented by characteristic doublets due to spin–orbit interaction with the splitting ΔE_{sl} of 1.1 and 10.8 eV [11], respectively. The lines of C 1*s*, O 1*s*, and N 1*s* electrons are singlets, but the spectra of these electrons exhibit a complex structure due to occurrence of ions in different oxidation states in the examined compounds and complexes (Figs. 2–4). The spectra of C 1*s* electrons con-

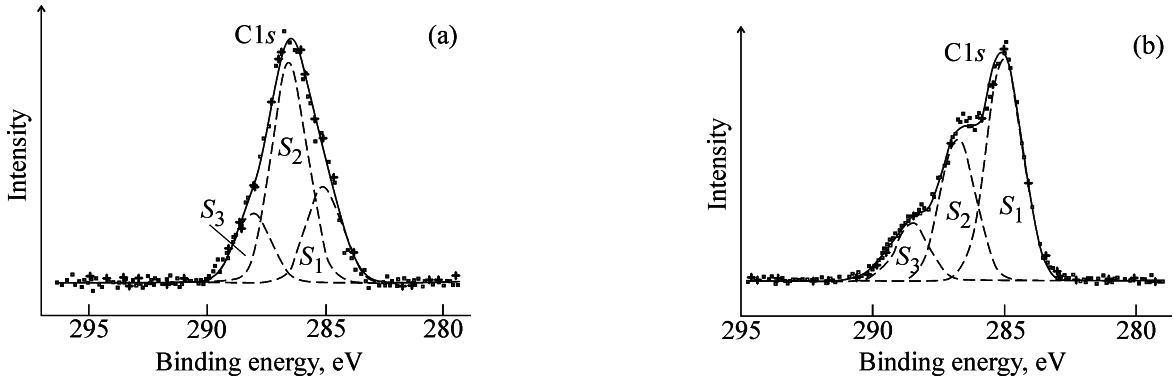

Fig. 2. X-ray photoelectron spectra of C1*s* electrons for sample nos. (a) 3a and (b) 1a.

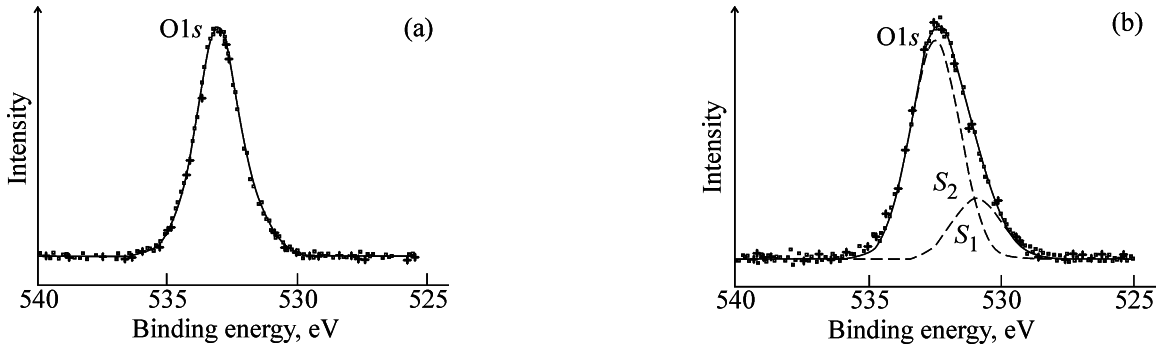

Fig. 3. X-ray photoelectron spectra of O1*s* electrons for sample nos. (a) 3a and (b) 4.

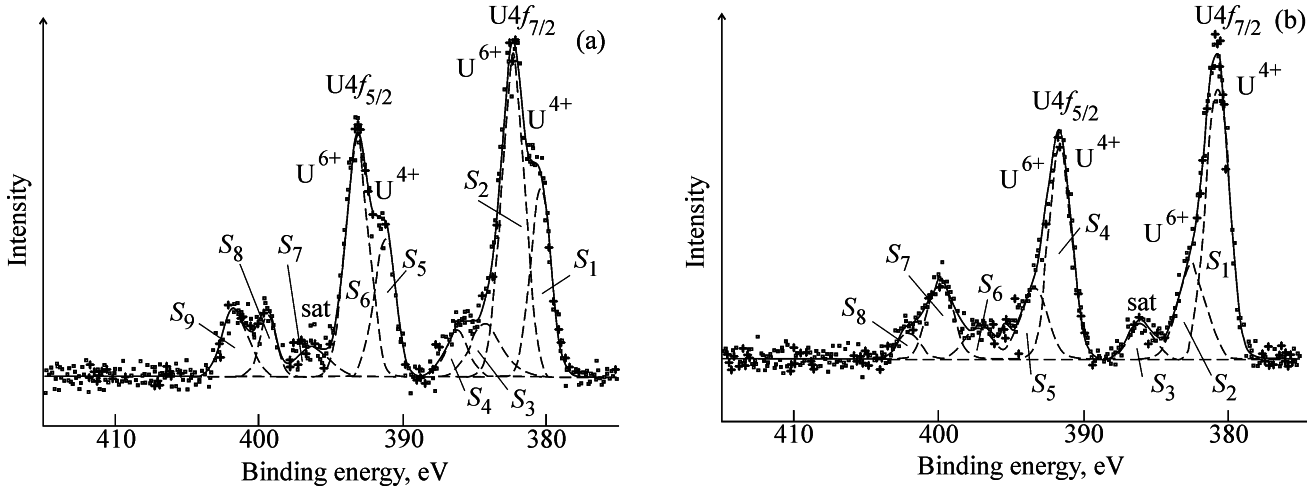

Fig. 4. X-ray photoelectron spectra of U4*f* and N1*s* electrons for sample nos. (a) 1a and (b) 1b.

tain a number of lines associated with different oxidation states of C (Fig. 2a). This spectrum allows only qualitative assignment of the lines to the specific C atoms in the polymer. For example, the line at 285.0 eV should be attributed to saturated C atoms (e.g., $-CH_3$); that at 286.7 eV, to C atoms bound to the O atom; and that at 288.4 eV, to C atoms bound to two O atoms. The spectrum of C1*s* electrons of powdered chitosan also contains three lines, among which the middle line more than twice surpasses in intensity the two other lines. Notably, the spectra of C1*s* electrons remained unchanged with the time of residence of the sample in the spectrometer.

The spectrum of O1*s* electrons of powdered

chitosan (sample no. 3a) is represented by a fairly symmetrical narrow (Γ = 1.5 eV) line with a small shoulder on the lower-energy side. This shoulder can be attributed to the OH^- group. In the spectrum of the chitosan–U(VI) complex (sample no. 4) the low-energy shoulder increases in intensity, probably due to the appearance of additional hydroxy groups in the complex. A similar situation is observed for the X-ray photoelectron spectra of sample nos. 1 and 2.

The spectrum of O 1*s* electrons of the chitosan–U(VI) complex (sample no. 2) consists of two lines (see table and Fig. 4) at 531.3 and 533.1 eV. From the equation [14]

$$E_b\,(\text{eV}) = 2.27R_{M-O}^{-1}\,(\text{nm}) + 519.4 \quad (2)$$

follows

$$R_{M-O}\,(\text{nm}) = 2.27(E_b - 519.4)^{-1}. \quad (3)$$

Hence, the binding energy of O 1*s* electrons allows estimation of the length of the bond with oxygen R_{M-O}, nm, in the samples examined. These parameters were estimated at 0.191 and 0.166 nm. It should be noted that they characterize the lengths of bonds involving oxygen in chitosan and serve for estimation of their length [15].

For chitosan (sample no. 3), the spectrum of N 1*s* electrons observed at E_b = 399.7 eV (see table) is represented by one, relatively narrow (Γ = 1.3 eV) line. Complexation between chitosan and U(VI) (sample nos. 1, 2, and 4) is responsible for the appearance of an additional line at $E_b \approx 401.6$ eV in the spectrum of N 1*s* electrons on the higher-energy side. This line decreases in intensity with time, possibly due to cleavage of the U–N bond in the complexes examined.

The spectrum of chitosan (sample no. 3), within the accuracy, does not contain lines of S 2*p* electrons of sulfur. At the same time, the spectrum of the chitosan–U(VI) complex (sample no. 4) contains weak lines of S 2*p* electrons at 160.5 and 165.8 eV (see table). The high-energy line can be attributed to the SO_3^{2-} group, and the line at 160.5 eV, to sulfur participating in chemical bonding with other atoms [13].

The spectrum of U 4*f* electrons in $UO_2SO_4 \cdot nH_2O$ (sample no. 5) consists of a doublet of relatively narrow lines with shake-up satellites on the higher-energy side with 20% intensity, separated from the main lines by 2.8 eV (see table). The observed spectrum is typical for the U^{6+} ion [12]. The spectrum of U 4*f* electrons of the complex of uranium with chitosan film (sample no. 1) is indicative of two chemically nonequivalent states of uranium ions, U^{4+} and U^{6+} (Fig. 4a). With increasing time of residence of the sample in the spectrometer, the lines of the U^{4+} ions considerably grow in intensity (Fig. 4b). This is due to changes on the surface of the chitosan–U(VI) complex under high-vacuum exposure at room temperature. It can be presumed that, in the initial state, the complex contained U^{6+} ions solely.

Similar XPS spectra were observed for other chitosan–U(VI) complexes examined (sample nos. 2 and 4).

In quantitative elemental and ionic analyses of the examined samples of compounds and complexes, an increase in the error of measurement of the spectral line areas for inner electrons of metals is due to the additional structure in the spectra, associated with secondary electronic processes, multielectron excitation. The latter is responsible for the appearance of shake-up satellites on the higher-energy side of the main lines; hence, their intensity can be partly taken into account in the analysis (Fig. 4). All this can be responsible for an additional error in elemental and ionic analyses, which can exceed 10%. In this approximation, based on the X-ray photoelectron spectra, we carried out elemental and ionic quantitative chemical analyses of the surface (~5 nm) of the examined samples relative to one C atom. The results are as follows: sample no. 1a: $C_{1.00}O_{0.53}N_{0.06}(N_{0.037}, N_{0.023})U_{0.011}(U^{4+}_{0.004}, U^{6+}_{0.007})$; sample no. 1b: $C_{1.00}O_{0.50}N_{0.07}(N_{0.050}, N_{0.020}) \cdot U_{0.010}(U^{4+}_{0.007}, U^{6+}_{0.003})$; sample no. 2a: $C_{1.00}O_{0.60} \cdot N_{0.14}(N_{0.114}, N_{0.026})U_{0.010}(U^{4+}_{0.005}, U^{6+}_{0.005})$; sample no. 2b: $C_{1.00}O_{0.50}N_{0.13}(N_{0.120}, N_{0.010})U_{0.009}(U^{4+}_{0.007}, U^{6+}_{0.002})$; sample no. 3a: $C_{1.00}O_{0.54}N_{0.13}$; sample no. 3b: $C_{1.00}O_{0.54}N_{0.12}$; and sample no. 4: $C_{1.00}O_{0.53} \cdot N_{0.07}(N_{0.063}, N_{0.007})U_{0.007}(U^{4+}_{0.005}, U^{6+}_{0.002})S_{0.013} \cdot (SO_3^{2-})S_{0.015}$(S–A).

These data somewhat differ from those initially calculated for the bulk of the sample. The reason is that the XPS data are relevant to the structure of the surface of 5–10-nm-thick samples.

To summarize, interaction of chitosan with uranyl group yields complexes containing in the equatorial plane the nitrogen atom of the amino group and also, probably, oxygen atoms from the ring of chitosan and free hydroxy groups. Prolonged exposure of the chitosan–U(VI) complex in a vacuum

of the spectrometer results in cleavage of the bonds linking the uranyl group to the amino and hydroxy groups. This is responsible for formation of U(IV) compounds on the surface, with the surface depletion in OH groups.

ACKNOWLEDGMENTS

The study was financially supported by the Russian Foundation for Basic Research (project no. 06-04-08 291).

REFERENCES

1. *Chemistry of the Actinide Elements*, Katz, J.J., Seaborg, G.T., and Morss, L.R., Eds., London: Chapman and Hall, 1985, vol. 1. Translated under the title Katz, J.J., Seaborg, G.T., and Morss, L.R., *Khimiya aktinoidov*, Moscow: Mir, 1991, vol. 1. pp. 205–222.
2. Myasoedova, G.V. and Nikashina, V.A., *Ross. Khim. Zh.*, 2006, vol. 1, no. 5, pp. 55–63.
3. Muzarelli, R.A.A., *Natural Chelating Polymers: Alginic Acid, Chitin and Chitosan*, Oxford: Pergamon, 1973, p. 309.
4. Piron, E. and Domard, A., *Int. J. Biol. Macromol.*, 1997, vol. 21, pp. 327–335.
5. Piron, E. and Domard, A., *Int. J. Biol. Macromol.*, 1998, vol. 22, pp. 33–40.
6. *Khimiya urana* (Chemistry of Uranium), Laskorin, B.N., Ed., Moscow: Nauka, 1981, pp. 58–67.
7. Varma, A.J., Dashpande, S.V., and Kennedy, J.F., *Carbohydr. Polym.*, 2004, vol. 55, pp. 77–93.
8. Veleshko, A.N., Rumyantseva, E.V., Kulyukhin, S.A., et al., *Radiokhimiya*, 2008, vol. 50, no. 5, pp. 446–453.
9. Rumyantseva, E.V., Chernyshenko, A.O., Neborako, A.A., et al., Abstracts of Papers, *Vos'maya Mezhdunarodnaya konferentsiya "Sovremennye perspektivy v issledovanii khitina i khitozana"* (Eighth Int. Conf. "Modern Prospects in Chitin and Chitosan Studies"), Kazan: VNIRO, 2006, pp. 126–130.
10. *Practical Surface Analysis by Auger and X-ray Photoelectron Spectroscopy*, Briggs, D, and Seah, M.P., Eds., New York: Wiley, 1983.
11. Fuggle, J.C. and Martensson, N., *J. Electron Spectrosc. Relat. Phenom.*, 1980, vol. 21, pp. 275–281.
12. Teterin, Yu.A. and Teterin, A.Yu., *Usp. Khim.*, 2004, vol. 73, no. 6, pp. 25–27.
13. Nefedov, V.I., *Rentgenoelektronnaya spektroskopiya khimicheskikh soedinenii* (X-ray Photoelectron Spectroscopy of Chemical Compounds), Moscow: Khimiya, 1984.
14. Sosul'nikov, M.I. and Teterin, Yu.A., *Dokl. Akad. Nauk SSSR*, 1991, vol. 317, no. 2, pp. 418–421.
15. Wells, A.F., *Structural Inorganic Chemistry*, Oxford: Oxford Univ. Press, 1984.
16. Teterin, Yu.A., *NATO ASI-Ser., Biotechnology for Waste Management and Site Restoration*, Ser. 2: *Environment*, Ronneau, C. and Bitchaeva, O., Eds., New York: Kluwer Academic, 1997, vol. 34, pp. 135–139.